

Effects of incomplete superconducting condensation in *S*-wave superconductors

Ju. H. Kim

Department of Physics, University of North Dakota, P.O. Box 7129, Grand Forks, North Dakota 58202

(Received 17 May 1999; revised manuscript received 25 October 1999)

We have reexamined quasiparticle excitations in *s*-wave superconductors by considering a finite range T_d of pairing interaction energy. When T_d is finite, low-energy states which are believed to be a hallmark of other pairing symmetries such as *d*-wave symmetry are also found in *s*-wave superconductors. We have numerically computed (i) the quasiparticle density of states, (ii) the order parameter, (iii) the superfluid density as a function of T_d/T_c , and (iv) the critical temperature T_c as a function of effective coupling constant. These calculations show unusual features which arise as a result of these low-energy states when T_d becomes comparable to T_c . In conventional superconductors, where $T_d/T_c \gg 1$, the BCS results are recovered as the effect of the low-energy states becomes negligible.

The gap in the energy spectrum for quasiparticle excitation is known as a hallmark of weak-coupling *s*-wave superconductors.¹ Its presence in conventional superconductors has been seen in various experiments including measurements of the magnetic penetration depth, specific heat, and nuclear relaxation rate as the exponentially activated temperature, T , dependence^{1,2} at low T . For example, the T dependence of experimental data is found to be compatible with a gap in the energy spectrum of superconductors such as aluminum, vanadium, V_3Si , and niobium. However, it has been noticed that tunneling data^{3,4} for lanthanum and Nb_3Sn and specific heat data⁵ for V_3Si at low magnetic fields appear inconsistent with the BCS density of states (DOS). The T dependence of the specific heat for indium and the order parameter $\Delta(T)$ for niobium also show a deviation⁶ from the BCS results. These data suggest that low-energy states may be present below the energy gap.

The two energy scales which characterize these superconductors are the range T_d of pairing interaction energy and the critical temperature T_c . T_d corresponds to the Debye temperature in the phonon-mediated superconductors. The values of T_d/T_c for aluminum, vanadium, indium, V_3Si , niobium, lanthanum, and Nb_3Sn are $T_d/T_c \approx 356, 71, 32, 31, 30, 23$, and 16, respectively.⁷ This suggests that the appearance of low-energy states below the energy gap may be related to decreasing T_d/T_c . This also suggests the interesting possibility that the presence of an energy gap may *not* be a universal feature of *s*-wave superconductors, but may pertain only to the weak-coupling superconductors (i.e., $T_d/T_c \gg 1$). The possibility of low-energy states in *s*-wave superconductors was suggested recently by Nam.⁸

The origin of low-energy states is unpaired quasiparticles at $T=0$. Unpaired quasiparticles in superfluids can arise due to either the interactions⁹ between atoms or those that are being *left out* of pairing. When all quasiparticles participate in the pairing interaction, the single-valuedness boundary condition for the ground-state wave function can be used to show that the superfluid fraction approaches unity in the zero-temperature limit.¹⁰ However, when some quasiparticles do not participate in the pairing interaction, as in the case of spin-1 superfluid,¹¹ the superfluid fraction becomes less than unity at $T=0$, indicating that these quasiparticles

effectively form a normal component. Unpaired quasiparticles can be also present in superconductors at $T=0$. In superconductors, however, they are due to finite T_d .^{8,12} According to BCS theory, some fraction of the charge carriers can remain unpaired when T_d is finite because only electrons with (kinematic) energy within T_d of the Fermi surface can participate in the pairing interaction.^{2,12} When T_d is *infinite*, as in the conventional BCS calculations, no quasiparticles are unpaired, thus yielding an energy gap and the BCS DOS. In the BCS calculation, T_d is taken as *infinite* and a cutoff is imposed on the dynamical variable ω for convenience. However, this approach is not valid. As a result, the BCS calculation needs to be reexamined because T_d must be finite in order to obtain finite T_c . This finite T_d yields a correction¹² of order $\mathcal{O}(T_c/T_d)$ to the BCS results. Although this is negligible when $T_d/T_c \gg 1$, the correction should not be neglected when $T_d/T_c \sim 1$. Therefore, in contrast to weak-coupling superconductors, the low-energy states become significant in strong-coupling superconductors since the fraction of unpaired quasiparticles increases as $T_d/T_c \rightarrow 0$. This implies that a drastic modification of the conventional BCS results can arise when $T_d \sim T_c$. A modification of the conventional BCS results based on the notion of incomplete superconducting condensation due to finite T_d may provide insights into experimental phenomena that are not understood clearly and show deviations from the strict BCS limit. These phenomena include the anomalous temperature dependence of upper critical field,¹³ anomalous Hall effect,¹⁴ and the magnetic field dependence of the specific heat.⁵

In this paper, we reexamine the BCS calculation and determine the effect of finite T_d by imposing a cutoff on the energy. We discuss the DOS and show how, in contrast to general belief, the low-energy states arise in the calculation. To demonstrate the effect of finite T_d , we calculate microscopic quantities such as (i) the DOS $N_s(\omega)$, (ii) $\Delta(T)$, and (iii) the superfluid density $\rho_s(T)$ as a function of T_d/T_c . We also compute (iv) T_c as a function of effective coupling constant. Interestingly, the DOS for $T_d \sim T_c$ resembles the *d*-wave DOS at low ω , while the calculation recovers the BCS results as $T_d \rightarrow \infty$. Here T_d/T_c is varied from the weak-coupling to the strong-coupling regime. We note that it may

not be appropriate to apply this approach to an arbitrary T_d/T_c . In the strong-coupling regime, the results may need to be justified by using the Eliashberg equations.¹⁵ However, we believe the results presented here are qualitatively correct because they depend on only the low-energy states.

In most superconductors, the order parameter is usually anisotropic, but we consider an isotropic order parameter for simplicity. The self-consistency condition for the \mathbf{k} and ω dependence of the order parameter $\Delta_{\mathbf{k}}(\omega)$ is given by¹

$$\Delta_{\mathbf{k}}(\omega) = - \sum_{\mathbf{k}'} V_{\mathbf{k}\mathbf{k}'} \frac{\Delta_{\mathbf{k}'}(\omega)}{2E_{\mathbf{k}'}} \tanh \frac{E_{\mathbf{k}'}}{2T}, \quad (1)$$

where $E_{\mathbf{k}} = \sqrt{\epsilon_{\mathbf{k}}^2 + \Delta_{\mathbf{k}}^2(\omega)}$. We set $\hbar = k_B = c = 1$ for convenience. Within the BCS approximation, the condition of non-zero effective pairing interaction, $V_{\mathbf{k}\mathbf{k}'} = -V$, between electrons with energy $|\epsilon_{\mathbf{k}}| < T_d$ is satisfied by^{2,12}

$$\Delta_{\mathbf{k}}(\omega) = \begin{cases} \Delta(T) & \text{for } |\epsilon_{\mathbf{k}}| < T_d, \\ 0 & \text{for } |\epsilon_{\mathbf{k}}| > T_d, \end{cases} \quad (2)$$

for all frequencies ω . Here $\epsilon_{\mathbf{k}}$ is the quasiparticle energy for momentum \mathbf{k} in the normal state measured with respect to the Fermi energy. This cutoff reflects the fact that only the quasiparticles with energy $|\epsilon_{\mathbf{k}}|$ within T_d can form pairs.

(i) *Density of states*: The quasiparticle DOS normalized to the normal state single-spin DOS, $N(0)$, at the Fermi energy is determined from¹⁶

$$n(\omega) = \frac{N_s(\omega)}{N(0)} = \text{Im} \left\{ -\frac{1}{\pi} \int_{-\infty}^{\infty} d\epsilon_{\mathbf{k}} \frac{1}{2} \text{Tr}[G(\mathbf{k}, \omega)] \right\}, \quad (3)$$

where $G(\mathbf{k}, \omega) = [\omega \tau_0 - \Delta_{\mathbf{k}}(\omega) \tau_1 - \epsilon_{\mathbf{k}} \tau_3]^{-1}$ is the quasiparticle Green function in the superconducting state¹⁶ and τ_i is the i th Pauli matrix. Calculation of the DOS from Eq. (3) by evaluating the integral over $\epsilon_{\mathbf{k}}$ becomes straightforward in the weak-coupling limit because, by taking T_d as *infinite* as in the BCS calculation, the integration over $\epsilon_{\mathbf{k}}$ can be performed by residues. As a result of this integration, the BCS density of states¹

$$n_{\text{BCS}}(\omega) = \text{Re} \left\{ \frac{\omega}{\sqrt{\omega^2 - \Delta^2}} \right\} \quad (4)$$

is obtained. It is worth noting that the BCS expression of $T_c = 1.13T_d e^{-1/N(0)V}$ and the BCS DOS represent the treatment of T_d as finite and as infinite, respectively. Taking T_d as infinite leads to an error $\mathcal{O}(T_c/T_d)$ which is negligible in the weak-coupling regime.¹²

As a way to treat finite T_d consistently, Eq. (2) must be taken into account when computing the DOS by integrating over $\epsilon_{\mathbf{k}}$ in Eq. (3). When a cutoff is rigorously imposed on the energy, the usual approach of carrying out a residue integral is not useful because the pole of $G(\mathbf{k}, \omega)$ is a multi-valued function of ω . It should be also noted that, for finite T_d , another usual approach of computing the DOS via taking $d\epsilon_{\mathbf{k}}/dE_{\mathbf{k}}$ is not valid because $\epsilon_{\mathbf{k}}$ is not a single-valued function of $E_{\mathbf{k}}$. Moreover, $\Delta_{\mathbf{k}}(\omega)$ of Eq. (2) is a rapidly changing function of $\epsilon_{\mathbf{k}}$ near T_d .^{2,12}

One way to evaluate Eq. (3) taking Eq. (2) into account is by integrating $\epsilon_{\mathbf{k}}$ over two fan-shaped contours with real and imaginary axes in the $\epsilon_{\mathbf{k}}$ plane as shown in Fig. 1. These

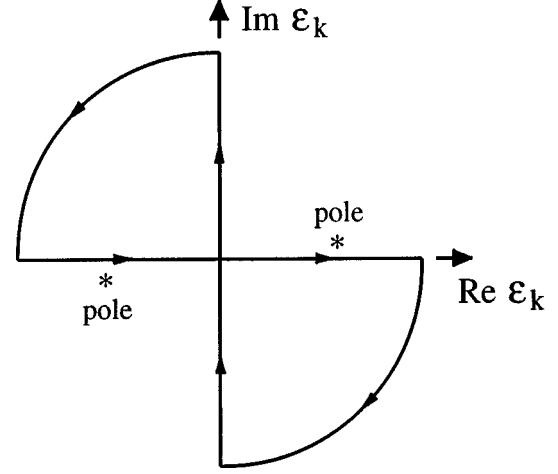


FIG. 1. Two fan-shaped contours for computing the DOS for finite T_d are schematically shown.

contours do not enclose the pole. As a result of this integration, the DOS has two terms

$$n(\omega) = \mathcal{Q}(\omega, T_d) + n_{\text{BCS}}(\omega) \mathcal{R}(\omega, T_d), \quad (5)$$

where $\mathcal{Q}(\omega, T_d) = (2/\pi) \tan^{-1}(\omega/T_d)$ and $\mathcal{R}(\omega, T_d) = (2/\pi) \tan^{-1}[n_{\text{BCS}}(\omega) T_d/\omega]$.⁸ The first and second terms correspond to the contributions from $|\epsilon_{\mathbf{k}}| > T_d$ and $|\epsilon_{\mathbf{k}}| < T_d$, respectively. In the limit of $T_d = \infty$, $n(\omega) = n_{\text{BCS}}(\omega)$. We note that the first term $\mathcal{Q}(\omega, T_d)$, which accounts for the low-energy states, does not depend on Δ . The presence of these low-energy states in the DOS may be understood in the following way. The states with energy less than Δ are shifted to higher energy as pairs are formed. When T_d is infinite, all states below Δ are shifted above Δ , yielding an energy gap which is described by $n_{\text{BCS}}(\omega)$. When T_d is finite, on the other hand, *not* all the states are shifted above Δ . The states remaining below Δ are the aforementioned low-energy states and represent the unpaired quasiparticles.

In Fig. 2, the DOS is plotted as a function of ω/Δ for $T_d/T_c = 160$ (dashed line), 3.1 (solid line), and 1.6 (dot-dashed line). For $T_d/T_c = 160$, only a very small fraction of the states is below Δ (i.e., $\omega < \Delta$) and, as a result, Δ appears as an energy gap. Hence the DOS for $T_d/T_c = 160$ is very similar to the BCS DOS. As T_d/T_c decreases, the DOS increases for $\omega < \Delta$ and decreases for $\omega > \Delta$ because the low-energy states (i.e., $\omega < \Delta$) that were shifted to higher energies (i.e., $\omega > \Delta$) become, again, low-energy states. The fraction of states below Δ increases with decreasing T_d/T_c , indicating that the effect of finite T_d becomes significant in strong-coupling superconductors. The DOS increases linearly with ω at low ω , suggesting that the ω dependence of the DOS for an s -wave superconductor may be similar to that in a d -wave superconductor¹⁷ when low-energy states are present. In the inset, $n(\omega) - n_{\text{BCS}}(\omega)$ is plotted as a function of ω/Δ for $T_d/T_c = 160$ (dashed line), 3.1 (solid line), and 1.6 (dot-dashed line) to illustrate the effect of finite T_d on the DOS for both above and below Δ . One can find that the areas under the $n(\omega) - n_{\text{BCS}}(\omega)$ curve for $\omega/\Delta < 1$ and for $\omega/\Delta > 1$ are equal and opposite, indicating that Eq. (5) satisfies the sum rule.

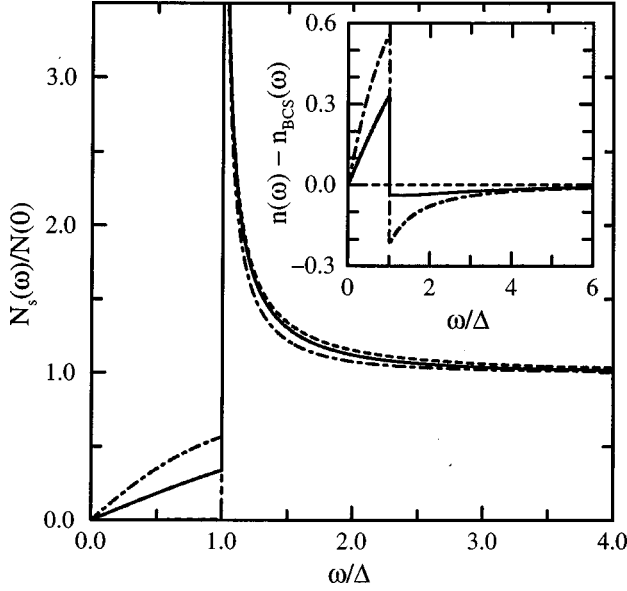


FIG. 2. The DOS plotted as a function of ω/Δ for $T_d/T_c = 160$ (dashed line), 3.1 (solid line), and 1.6 (dot-dashed line) shows the presence of low-energy states. The dashed line is very similar to the BCS DOS. In the inset, $n(\omega) - n_{\text{BCS}}(\omega)$ plotted as a function of ω/Δ for $T_d/T_c = 160$ (dashed line), 3.1 (solid line), and 1.6 (dot-dashed line) satisfies the sum rule.

(ii) *Order parameter*: The value of the order parameter $\Delta(T)$ depends also on T_d/T_c . The dependences of $\Delta(T)$ on T and T_d/T_c are determined from the BCS equation¹

$$\frac{1}{N(0)V} = \int_0^{T_d} \frac{d\epsilon_{\mathbf{k}}}{\sqrt{\epsilon_{\mathbf{k}}^2 + \Delta^2(T)}} \tanh \frac{\sqrt{\epsilon_{\mathbf{k}}^2 + \Delta^2(T)}}{2T}. \quad (6)$$

In Fig. 3, the value of $2\Delta(0)/T_c$ computed numerically from Eq. (6) is plotted as a function of T_d/T_c . This curve illus-

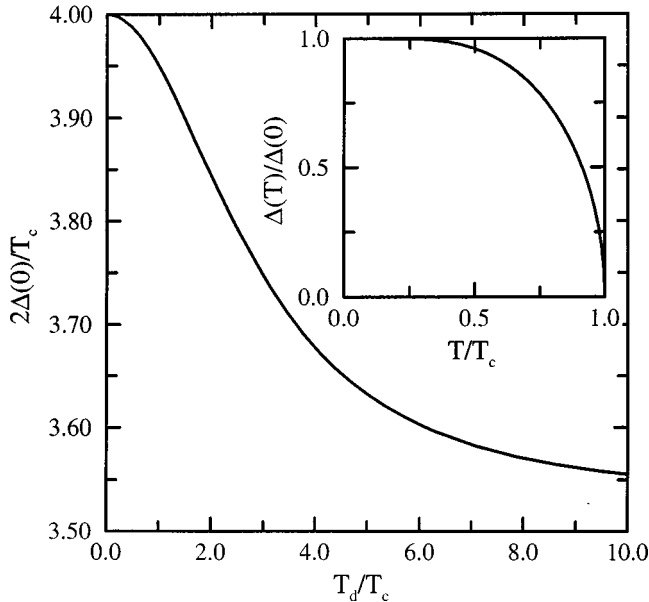


FIG. 3. The order parameter at $T=0$ is plotted as a function of T_d/T_c to show a deviation from the BCS value of $2\Delta(0)/T_c = 3.527$. In the inset, a universal function $\Delta(T)/\Delta(0)$ is plotted as a function of T/T_c .

trates the fact that a deviation from the BCS value of $2\Delta(0)/T_c = 3.527$ can arise when T_d is finite. As T_d/T_c decreases, $2\Delta(0)/T_c$ increases^{18,19} slowly in the weak-coupling regime from the BCS value at $T_d = \infty$ and then increases rapidly in the strong-coupling regime. The maximum value for $2\Delta(0)/T_c$ is 4 at $T_d/T_c = 0$. This value is in agreement with the result obtained analytically.²⁰ The value of $2\Delta(0)/T_c$ obtained from the tunneling data for aluminum, vanadium, indium, $V_3\text{Si}$, niobium, lanthanum, and Nb_3Sn is 3.5, 3.5, 3.68, 3.8, 3.89, 3.75, and 4.3, respectively.⁷ From these superconductors, it can be easily seen that a qualitative trend of increasing $2\Delta(0)/T_c$ with decreasing T_d/T_c is consistent with the present calculation. However, the quantitative agreement between the computed and the measured value for $2\Delta(0)/T_c$ is poor. This may be due to the anisotropic effect which may become progressively more important with decreasing T_d/T_c . In the inset, the computed $\Delta(T)/\Delta(0)$ is plotted as a function of T/T_c . The $\Delta(T)/\Delta(0)$ curve does not depend on T_d/T_c , indicating that it is a universal function of T/T_c .²

(iii) *Superfluid density*: Due to the presence of unpaired quasiparticles, the superfluid fraction $\rho_s(0)/\rho$ at $T=0$ depends on T_d/T_c . The dependence of $\rho_s(0)/\rho$ on T_d/T_c can be determined from the $\mathcal{Q}(\omega, T_d)$ term in the DOS of Eq. (5) by using

$$\frac{\rho_s(0)}{\rho} = 1 - \frac{1}{\Delta(0)} \int_0^{\Delta(0)} d\omega \mathcal{Q}(\omega, T_d), \quad (7)$$

where ρ is the carrier density.⁸ The T dependence of $\rho_s(T)$ can be determined^{16,21} from the electromagnetic response function $\mathcal{K}(\mathbf{q}, \omega)$ in the limit of $\mathbf{q} = \omega = 0$ via the relation $\mathcal{K}(0,0)|_T / \mathcal{K}(0,0)|_{T=0} = \rho_s(T)/\rho_s(0)$. The $\rho_s(T)$ normalized by $\rho_s(0)$ can be written as

$$\frac{\rho_s(T)}{\rho_s(0)} = 1 - \frac{2}{T} \int_0^\infty d\omega n(\omega) f(\omega) [1 - f(\omega)], \quad (8)$$

where $f(\omega) = 1/(e^{\omega/T} + 1)$ is the Fermi function.

In Fig. 4, the computed $\rho_s(0)/\rho$ from Eq. (7) is plotted as a function of T_d/T_c to show the fraction of quasiparticles not participating in pairing. We note that $\rho_s(0)/\rho$ deviates from the BCS value of 1 due to unpaired quasiparticles which are represented as the low-energy states in Fig. 2. As T_d/T_c decreases, $\rho_s(0)/\rho$ decreases from 1 at $T_d/T_c = \infty$, reflecting the increase in the fraction of unpaired quasiparticles. We note that $\rho_s(0)/\rho \rightarrow 0$ as $T_d/T_c \rightarrow 0$, indicating that all quasiparticles are unpaired when $T_d = 0$, as should be expected. In the inset, $\rho_s(T)/\rho_s(0)$ is plotted as a function of T/T_c for $T_d/T_c = 160$ (dashed line), 3.1 (solid line), and 1.6 (dot-dashed line) to illustrate the T dependence of $\rho_s(T)$. The dashed line is very similar to the BCS result. For $T_d/T_c = 3.1$ and 1.6, $\rho_s(T)/\rho_s(0)$ decreases linearly with T at low T , reflecting the linear ω dependence of the DOS of Eq. (5) at low ω .

(iv) *Critical temperature*: The dependence of T_c on the effective coupling constant is determined from

$$\frac{1}{N(0)V} = \int_0^{T_d} \frac{d\epsilon_{\mathbf{k}}}{\epsilon_{\mathbf{k}}} \tanh \frac{\epsilon_{\mathbf{k}}}{2T_c}. \quad (9)$$

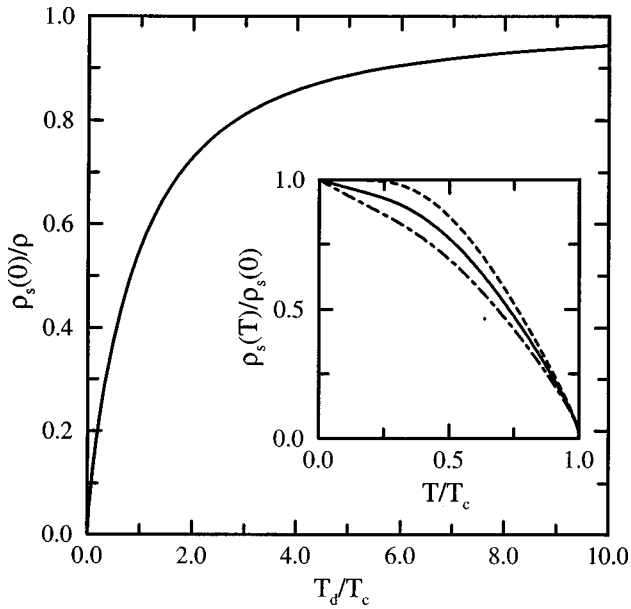


FIG. 4. The superfluid fraction $\rho_s(0)/\rho$ at $T=0$ plotted as a function of T_d/T_c shows that a deviation from the BCS value of 1 arises due to the presence of unpaired quasiparticles in the superconducting state. In the inset, $\rho_s(T)/\rho_s(0)$ plotted as a function of T/T_c for $T_d/T_c=160$ (dashed line), 3.1 (solid line), and 1.6 (dot-dashed line) represents the low-energy states in Fig. 2. The dashed line is very similar to the BCS result.

In Fig. 5, the computed T_c (solid line) from Eq. (9) and the BCS expression for T_c (dashed line), which is obtained by assuming $N(0)V \ll 1$, are plotted as a function of $N(0)V$ in order to illustrate the difference between the numerically computed T_c and the BCS result in the strong-coupling regime. Two curves almost coincide for $N(0)V \ll 1$ (i.e., weak coupling), but the difference between these curves increase with increasing $N(0)V$ and this difference becomes significant for $N(0)V > 1$ (i.e., strong coupling).

In summary, we have determined the effect of finite T_d within the BCS pairing theory by rigorously imposing a cut-off on the (kinematic) energy. Numerical calculations of (i) the DOS, (ii) $\Delta(T)$, and (iii) $\rho_s(T)$ as a function of T_d/T_c and (iv) T_c as a function of $N(0)V$ indicate that the BCS results are recovered only when $T_d = \infty$. These computations show unusual features suggesting that the BCS results should

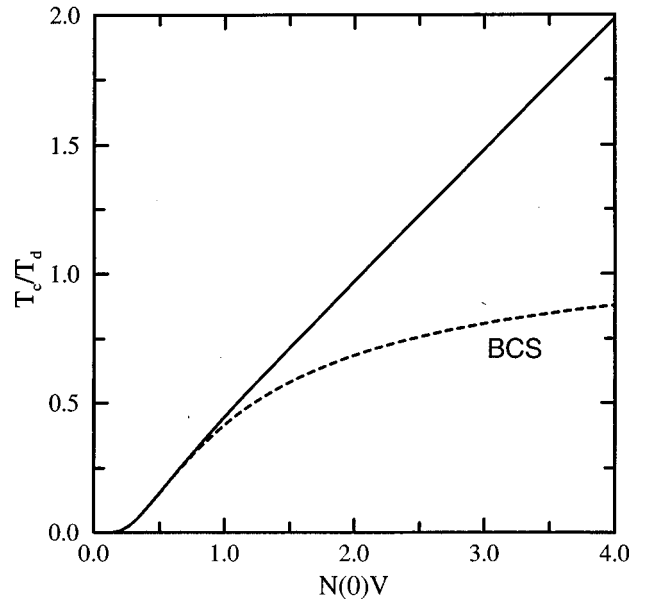


FIG. 5. The T_c/T_d curve plotted as a function of $N(0)V$ shows that the numerically calculated T_c (solid line) from Eq. (9) and the BCS expression for T_c (dashed line) almost coincide when $N(0)V \ll 1$, but are different when $N(0)V > 1$.

not be applied when T_d is comparable to T_c because a correction due to finite T_d is not negligible. An important consequence of a finite T_d is that unpaired quasiparticles can exist in an s -wave superconductor at $T=0$. These unpaired quasiparticles yield low-energy states, suggesting that an energy gap is not a universal feature of s -wave superconductors. The presence of low-energy states can change the T dependence of physical properties at low T , indicating that an s -wave superconductor may appear similar to a d -wave superconductor²² when T_d is comparable to T_c . Finally, we note that the present reexamination of the BCS calculations is based on the assumption that Migdal's theorem²³ is valid. However, when the vertex corrections are not negligible, the effects of incomplete condensation as presented in this work, which is based on the mean-field theory, may need to be reexamined.

The author is grateful to S. B. Nam for helpful suggestions and discussions.

¹J. Bardeen, L. N. Cooper, and J. R. Schrieffer, Phys. Rev. **108**, 1175 (1957).

²M. Tinkham, *Introduction to Superconductivity* (McGraw-Hill, Singapore, 1996).

³A. S. Edelstein, Phys. Rev. **180**, 505 (1969).

⁴Y. Goldstein, Rev. Mod. Phys. **36**, 213 (1964).

⁵A. P. Ramirez, Phys. Lett. A **211**, 59 (1996).

⁶R. Meservey and B. B. Schwarz, in *Superconductivity*, edited by R. D. Parks (Dekker, New York, 1969), p. 117.

⁷E. L. Wolf, *Principles of Electron Tunneling Spectroscopy* (Oxford University Press, New York, 1985), pp. 523–530.

⁸S. B. Nam, Phys. Lett. A **193**, 111 (1994); **197**, 458(E) (1995).

⁹See, for example, A. D. B. Woods and R. A. Cowley, Rep. Prog. Phys. **36**, 1135 (1973).

¹⁰A. J. Leggett, J. Stat. Phys. **93**, 927 (1998).

¹¹A. G. K. Modawi and A. J. Leggett, J. Low Temp. Phys. **109**, 625 (1997).

¹²A. A. Abrikosov, L. P. Gor'kov, and I. E. Dzyaloshinski, *Methods of Quantum Field Theory in Statistical Physics* (Dover, New York, 1963).

¹³See, for example, V. F. Gantmakher *et al.*, Phys. Rev. **54**, 6133 (1996); S. V. Shulga *et al.*, Phys. Rev. Lett. **80**, 1730 (1998).

¹⁴See, for example, A. W. Smith *et al.*, Phys. Rev. B **49**, 12 927 (1994); K. Noto, S. Shinzawa, and Y. Muto, Solid State Commun. **18**, 1081 (1976).

- ¹⁵G. M. Eliashberg, Zh. Eksp. Teor. Fiz **38**, 966 (1960) [Sov. Phys. JETP **11**, 696 (1960)]; **39**, 1437 (1961) [**12**, 1000 (1961)].
- ¹⁶J. R. Schrieffer, *Theory of Superconductivity* (Benjamin/Cummings, Reading, MA, 1964).
- ¹⁷T. Xiang and J. Wheatly, Phys. Rev. B **51**, 11 721 (1995).
- ¹⁸B. Muhlschlegel, Z. Phys. **155**, 313 (1959).
- ¹⁹J. C. Swihart, IBM J. Res. Dev. **6**, 14 (1962).
- ²⁰D. J. Thouless, Phys. Rev. **117**, 1256 (1960).
- ²¹S. B. Nam, Phys. Rev. **167**, 470 (1967).
- ²²D. J. Scalapino, Phys. Rep. **250**, 329 (1995).
- ²³A. B. Migdal, Zh. Eksp. Teor. Fiz **34**, 1438 (1958) [Sov. Phys. JETP **7**, 996 (1958)].